Origin of charge separation in III-nitride nanowires under strain

Yelong Wu,[1,2,3,a)] Guangde Chen,[1] Su-Huai Wei,[2] Mowafak M. Al-Jassim,[2] and Yanfa Yan[4]
[1]*MOE Key Laboratory for Nonequilibrium Synthesis and Modulation of Condensed Matter, Xi'an Jiaotong University, Xi'an, Shaanxi 710049, China*
[2]*National Renewable Energy Laboratory, Golden, Colorado 80401, USA*
[3]*Renewable and Sustainable Energy Institute, University of Colorado at Boulder, Boulder, Colorado 80309, USA*
[4]*Department of Physics and Astronomy, The University of Toledo, Toledo, Ohio 43606, USA*

(Received 28 October 2011; accepted 7 December 2011; published online 28 December 2011)

The structural and electronic properties of BN, AlN, and GaN nanowires (NWs) under different strain condition are investigated using first-principles calculations. We found an anomaly of band gap change with respect to the applied external uniaxial strain. We show that this is due to the band crossing caused by the crystal field splitting at the top of the valance band. Due to the difference of the atomic relaxation at the core and surface regions of the NW, we show that electron and hole separation can be achieved when the compressive uniaxial strain exceeds the critical value $|\epsilon_c|$. © *2011 American Institute of Physics*. [doi:10.1063/1.3673323]

In the last decade, group III nitride semiconductors have emerged as the most important material systems for light emission in the green, blue, and ultraviolet regions that were previously not accessible for efficient and stable solid-state lighting.[1–4] Forming nanostructures of these materials, especially nanowires (NWs), which possess unique physical and chemical properties arising from the large surface to volume ratio and the quantum confinement effects of the one-dimensional system, provides further opportunities of using them to design optoelectronic devices, nanoswitches, and nanocontacts.[5–8] In device design and fabrication, it is often desirable that the electrons and holes generated in the NWs can naturally separate to reduce the wavefunction overlap between them, thus the recombination rate. For example, making the electron and hole diffuse in different pathes after photoexcitation is an often used approach in improving the efficiency of a number of renewable energy applications, including hydrogen generation via photoelectrochemical water splitting[9] and solar cells.[10,11] Increased efforts have been devoted to search for realistic methods for efficient charge separation, and one of the approaches could be to form a type-II core/shell heterostructure NW where the holes and electrons travels in the core or shell regions, respectively.[12,13] Although this approach have some achievements, the core/shell NWs are often difficult to fabricate for materials with type-II band alignment. Thus, it is desirable to find a simple approach to obtain homo structures with simultaneous charge separation properties similar to those of core/shell heterostructures.

Properties of semiconductor nanostructures can be tuned by varying their size and shape. Because the surface and core regions of the nanostructure react differently to the external force or field, we may expect that it is possible to achieve charge separation in a pure nanostructure by morphology control. Indeed, it has been reported recently that significant modification of band structures and axial charge separation in silicon NWs can be achieved via uniaxial tensile and compressive deformation.[14–17] Therefore, applying strain in nitride NWs may also lead to charge separation in the NWs. However, the strain effect on properties of nitride NWs is still poorly understood.

In this letter, the structural and electronic properties of BN, AlN, and GaN NWs under different strain conditions are investigated using first-principles calculations. The band gaps for these nitride NWs show nonlinear relationship with the strain, and more interestingly, the slope of the band gap vs. strain curve changes sign at a critical compressive condition. We show that this is due to the band crossing caused by the crystal field splitting at the top of the valence band. Moreover, we find that charge separation of electron and hole states can also be controlled by applying external strain on the nitride NWs along the wire axis.

In our study, all the structural optimizations and energy band calculations are performed using the density-functional theory in the generalized-gradient approximation (GGA).[18] The projected augmented wave method (PAW)[19] as implemented in the VASP (Refs. 20 and 21) code is employed. The energy cutoff is set at 450 eV and a $1 \times 1 \times 6$ k-point grid is used for structural optimizations. All NWs are fully relaxed until the force acting on each atom is less than 0.02 eV/Å.

The atomic structures of all the NWs are initially constructed from the bulk wurtzite crystal structure with theoretically optimized lattice parameters. The direction of the NWs is chosen to be along the [0001] direction with six $(10\bar{1}0)$ lateral facets without passivation.[22,23] The supercell has a square shape in the xy plane with 108 atoms in it. A vacuum region of about 10 Å is set to decouple the interaction between adjacent NWs. In this work, we mainly focus on uniaxial strain applied to the NWs along the wire axis z and the strain is defined as $\epsilon = (c - c_0)/c_0$, where c is the NW lattice constant and c_0 is the equilibrium lattice constant of the NW. For each strain applied in the z direction, the atoms are allowed to fully relax within the strained unit cell by minimizing the total energy.

We first investigate the structural properties of all the NWs under different strain conditions. The results for AlN

a)Electronic mail: yelong.wu@stu.xjtu.edu.cn.

TABLE I. Structural properties of AlN NW under different strain conditions. d_z (Å) and d_{xy} (Å) are the average bond lengths along the z direction and away from the z direction, respectively; a (Å), c/a, and u are the structural parameters that gives the same bond lengths in a wurtzite structure; Δ_{CF} (eV) is the corresponding crystal field splitting for the wurtzite structure [$\Delta_{CF} = E(\Gamma_6) - E(\Gamma_1)$]. For ideal c/a ratio, in wutzite structure, $c/a = 1.633$.

Region	ϵ	d_z	d_{xy}	a	c/a	u	Δ_{CF}
Core	−8%	1.890	1.904	3.210	1.448	0.4065	−1.001
	−4%	1.900	1.906	3.174	1.529	0.3915	−0.5951
	0%	1.925	1.914	3.146	1.606	0.3808	−0.1746
	4%	1.972	1.919	3.123	1.683	0.3751	0.1765
	8%	2.035	1.924	3.108	1.756	0.3728	0.4541
surface	−8%	1.831	1.875	3.133	1.484	0.3938	−0.7642
	−4%	1.828	1.877	3.081	1.575	0.3767	−0.1906
	0%	1.841	1.885	3.041	1.662	0.3643	0.3881
	4%	1.865	1.894	3.002	1.751	0.3547	0.9655
	8%	1.904	1.904	2.972	1.837	0.3487	1.475

NW is shown in Table I. The trend for GaN and BN are similar. It is clear that under free strain condition, Al-N bond lengths on the surface layer (the outermost Al-N layer) is reduced due to the reduced coordination number, while in the core region (the innermost Al-N layer), they are less affected by the reduced dimensional and remain close to their original bulk value. Consequently, to have the same c value in the two regions, the effective c/a ratio at the surface is much larger than that at the core region. When we compress (negative strain) the NW along the z direction, all of the bond lengths decrease monotonically near-linearly. However, the bond lengths away from the z direction, d_{xy}, of the surface shell have a less shrinkage, so the c/a ratio decrease faster in the surface region. On the contrary, when a tensile strain is applied, the increase of the c/a ratio in the surface region is also faster than in the core region. The dependence of the c/a ratio on the strain is almost linear with the surface region having a larger slope. These can be understood by considering that surface bonds have larger freedom to relax in order to accommodate the strain.

Figure 1 displays the electronic band structures of the NWs under different strain, and the energy changes of the conduction band minimum (CBM), valance band maximum (VBM), and band gap as functions of strain. The charge density of the states around the VBM and CBM of the AlN NWs in a small given energy rang (e.g., 0.03 eV) under different strain conditions as well as BN and GaN NWs under −8% strain condition are presented in Fig. 2.

The band structures and charge density plots indicate that (1) under tensile strain (ϵ is positive), the energies of CBM and VBM states of the considered NWs shift in opposite directions in response to the applied strain, i.e., CBM (VBM) shifts downwards (upward) with increasing strain. (2) When the NW is compressed (ϵ is negative), the CBM goes up almost linearly with the increasing of the compressive strain, while the change of VBM is not monotonic. At first, the energy of VBM state decreases as the compressive strain increases. However, for large compressive strain, it will increase with the increase of the compressive strain. (3) Because the energy of the VBM state varies non-monotonically with the strain, the slope of the band gap vs. strain curve changes sign at a critical compressive condition, ϵ_c, which is similar for GaN and AlN but larger for the more covalent BN. (4) Under zero strain, the band edge states around the VBM and CBM are mainly localized on the surface layer. Interestingly, however, as the compressive strain increases, the CBM state becomes even more localized at the surface region but the VBM state becomes more localized in the core region. Consequently, well-separated electron and hole states, i.e., charge separation is realized.

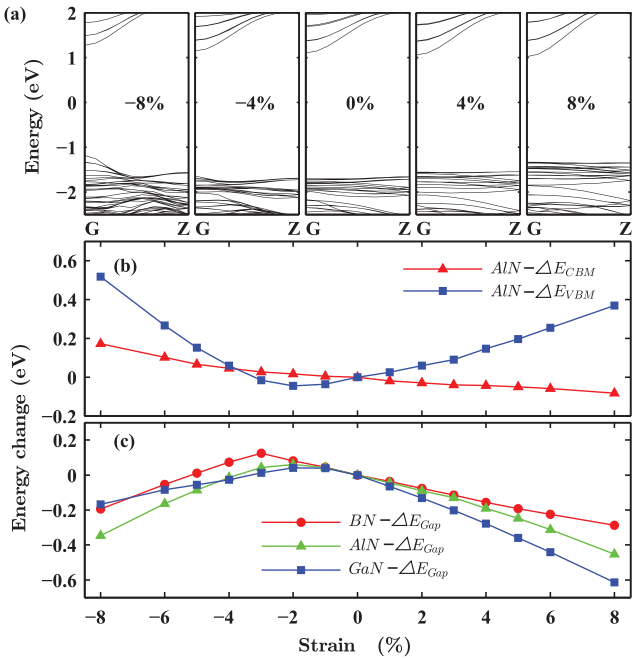

FIG. 1. (Color online) Electronic properties of the NWs under different strain condition: (a) near-gap band structures of AlN NW. An alignment has been done by using the core level; (b) the energy change of VBM and CBM of AlN NW as functions of strain; (c) the energy change of band gap vs. strain for BN, AlN, and GaN NWs.

The almost linear relationship between the energy change of CBM state and the strain can be easily understood by the deformation potential of the CBM state, which is an antibonding cation s and anion s state and depends mainly on the volume change.[24] When the strain decreases (becoming

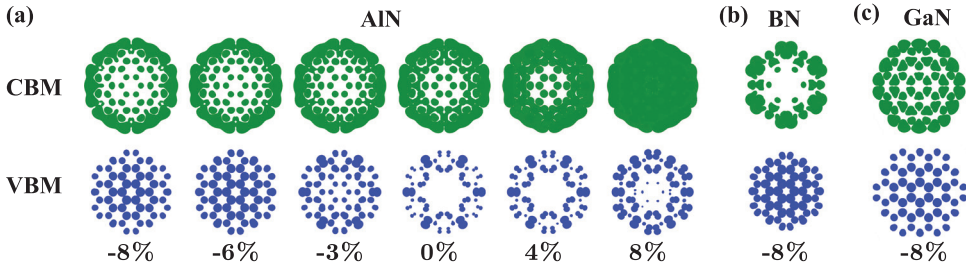

FIG. 2. (Color online) Charge density isosurfaces of states around the VBM and CBM of the NWs in a given energy rang of 0.03 eV. (a) AlN NW under different strain condition. (b) and (c) are for BN and GaN NWs, respectively, under −8% strain. The isosurfaces are 5% of the maximum values.

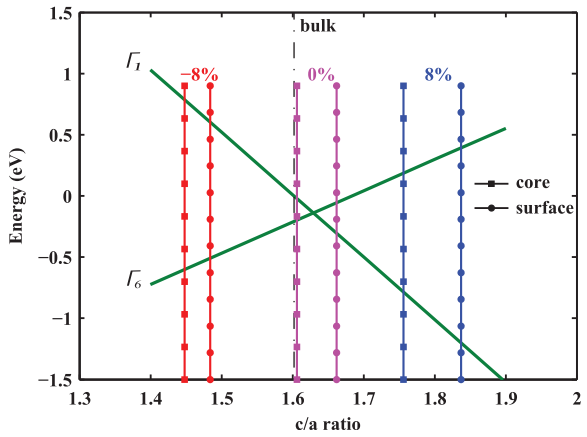

FIG. 3. (Color online) The effective c/a ratio and the corresponding VBM levels due to the crystal field splitting at surface (circle lines) and core regions (square lines) under different strain conditions.

more negative), the volume of the cell decreases, so the antibonding energy of the CBM increases. For the VBM state, it is mainly a bonding anion p and cation p state, so when the volume decreases, the volume deformation potential pushes the level down. But, there are three p state and under uniaxial strain these states will split. The crystal field splitting can be seen clearly from the band structures plotted in Fig. 1(a). Further analysis indicates that the anomaly of VBM change as a function of strain can be attributed to the combined effects of the volume deformation potential and the crystal field splitting. Specifically, when the NW has a tensile strain, due to the crystal field splitting, which depends almost linealy on the c/a ratio, the top of the VBM has the e-like symmetry (Γ_6 symmetry in wurtzite structure) and increases in energy with the tensile strain increases (see Fig. 3). Combined with the volume deformation potential, the VBM increases. Because the surface region has larger effective c/a ratio (i.e., more effective positive strain, see Table I), the states near the VBM are more localized on the surface. When the NW is compressed, the VBM will drop down due to the volume deformation potential, but will increase due to the crystal field splitting when the top of the VBM becomes a_1-like state (Γ_1 in wurtzite structure). Because the volume deformation potential is relatively small for more ionic AlN, GaN, as well as BN, the net effect is that the VBM will increase when the compressive strain increases (more negative). Because the core region has smaller effective c/a ratio (i.e., more effective negative strain, see Table I), the states near the VBM become more localized on the core region when high compressive strain is applied. For the CBM state, when it is compressed, the CBM in the core region feels higher pressure than that in the surface region, which pushes the CBM level in the core region even higher in energy than that in the surface region, therefore, it becomes more localized in the surface region when compressive strain is applied.

The explanation described above can also be used to explain the chemical trend of the critical strain $|\epsilon_c|$ observed for the three nitrides NWs. BN is more covalent than GaN and AlN, consequently, has large positive crystal filed splitting (0.267 eV, i.e., Γ_6 is above Γ_1, in wurtzite BN), therefore, it requires large $|\epsilon_c|$ to convert it to a negative crystal field splitting system. Although AlN has negative crystal field splitting in the bulk phase, the effective c/a value of AlN NW is large at surface due to its higher ionicity, which explains why it has similar $|\epsilon_c|$ as GaN, although GaN has slightly positive crystal field splitting in the bulk phase.

In summary, using first-principles calculations, we have investigated the structural and electronic properties of BN, AlN, and GaN nanowires along [0001] direction with the $\{10\bar{1}0\}$ lateral facets under different strain levels. An interesting non-monotonic change of the band gap vs. the uniaxial strain is observed. We find that it is caused by the switching of the crystal field splitted states at the VBM. Moreover, we predict that a separation of charge carriers with hole in the core region and electron at the surface region can be induced when the compressive strain exceeds the critical value $|\epsilon_c|$. These interesting behavior provides new opportunities for developing NW-based nano optoelectronic devices for renewable energy applications.

Y. Wu and G. Chen gratefully acknowledge the financial support of the China National Natural Science Fund (Grant Nos. 11074200 and 61176079). Y. Yan acknowledges the support from the Ohio Research Scholar Program (ORSP). The work at NREL is supported by the U.S. Department of Energy under Grant No. DE-AC36-08GO28308.

[1]F. A. Ponce and D. P. Bour, Nature **386**, 351 (1997).
[2]G. Fasol, Science **278**, 1902 (1997).
[3]P. Waltereit, O. Brandt, A. Trampert, H. T. Grahn, J. Menniger, M. Ramsteiner, M. Reiche, and K. H. Ploog, Nature **406**, 865 (2000).
[4]Y. Taniyasu, M. Kasu, and T. Makimoto, Nature **441**, 325 (2006).
[5]D. Appell, Nature **419**, 553 (2002).
[6]Y. Huang, X. Duan, Y. Cui, and C. M. Lieber, Nano Lett. **2**, 101 (2002).
[7]J. C. Johnson, H. J. Choi, K. P. Knutsen, R. D. Schaller, P. D. Yang, and R. J. Saykally, Nature Mater. **1**, 106 (2002).
[8]Y. J. Dong, B. Z. Tian, T. J. Kempa, and C. M. Lieber, Nano Lett. **9**, 2183 (2009).
[9]K. Fujii, T. K. Karasawa, and K. Ohkawa, Jpn. J. Appl. Phys., Part 2 **44**, L543 (2005).
[10]Q. W. Jiang, G. R. Li, and X. P. Gao, Chem. Commun., 6720 (2009).
[11]C. J. Neufeld, N. G. Toledo, S. C. Cruz, M. Iza, S. P. DenBaars, and U. K. Mishra, Appl. Phys. Lett. **93**, 143502 (2008).
[12]F. Qian, Y. Li, S. Gradecak, D. L. Wang, C. J. Barrelet, and C. M. Lieber, Nano Lett. **4**, 1975 (2004).
[13]H. M. Lin, Y. L. Chen, J. Yang, Y. C. Liu, K. M. Yin, J. J. Kai, F. R. Chen, L. C. Chen, Y. F. Chen, and C. C. Chen, Nano Lett. **3**, 537 (2003).
[14]A. J. Lu, R. Q. Zhang, and S. T. Lee, Appl. Phys. Lett. **91**, 263107 (2007).
[15]K. H. Hong, J. Kim, S. H. Lee, and J. K. Shin, Nano Lett. **8**, 1335 (2008).
[16]Z. G. Wu, J. B. Neaton, and J. C. Grossman, Nano Lett. **9**, 2418 (2009).
[17]A. Nduwimana and X. Q. Wang, J. Phys. Chem. C **114**, 9702 (2010).
[18]J. P. Perdew and Y. Wang, Phys. Rev. B **45**, 13244 (1992).
[19]P. E. Blochl, Phys. Rev. B **50**, 17953 (1994).
[20]G. Kresse and J. Furthmuller, Comput. Mater. Sci. **6**, 15 (1996).
[21]G. Kresse and J. Furthmuller, Phys. Rev. B **54**, 11169 (1996).
[22]Y. L. Wu, G. D. Chen, H. G. Ye, Y. Z. Zhu, and S.-H. Wei, J. Appl. Phys. **104**, 084313 (2008).
[23]Y. L. Wu, G. D. Chen, H. G. Ye, Y. Z. Zhu, and S.-H. Wei, Appl. Phys. Lett. **94**, 253101 (2009).
[24]Y. H. Li, X. G. Gong, and S.-H. Wei, Phys. Rev. B **73**, 245206 (2006).